The solubility of thorium in carbonate-bearing solutions at hydrothermal conditions

Haylea Nisbet*[1,2], Artas A. Migdisov[1], Anthony E. Williams-Jones[2], Vincent J. van Hinsberg[2], Hongwu Xu[1], Robert Roback[1]

[1]Earth and Environmental Sciences Division, Los Alamos National Laboratory, Los Alamos, New Mexico, 87545, USA.

[2]Department of Earth and Planetary Sciences, McGill University, 3450 University Street, Montreal, Quebec, H3A 0E8, Canada.

corresponding author: haylea.nisbet@mail.mcgill.ca

Abstract

Thorium mineralization is frequently hosted in carbonate-bearing rocks, and thorium commonly substitutes into the structures of carbonate-bearing minerals that have precipitated from or been modified by hydrothermal fluids. Given this common association, it is reasonable to consider the hypothesis that the presence of carbonate ligands in hydrothermal solutions promotes the transport of Th through the formation of stable aqueous complexes. Our ability to evaluate this hypothesis, however, is hindered by the lack of experimental data for Th-carbonate species at conditions beyond ambient. The low-temperature data indicate that carbonate is a strong complexing agent for Th. In this contribution, we investigate the solubility of Th in carbonate-bearing fluids relevant to natural systems (0.05-0.5m $NaHCO_3/Na_2CO_3$; pH_T ~7.8-9.8) at elevated temperature (175-250°C). We demonstrate that, in contrast to the behavior of Th at low temperature, the stability of Th-carbonate complexes is not sufficient for them to predominate at these conditions. Instead, the solubility of Th is governed by hydrolysis reactions. Under the experimental conditions investigated, the predominant hydroxyl complexes are $Th(OH)_4^0$ and $Th(OH)_5^-$. Thermodynamic formation constants were derived for these species at the temperatures

Nisbet, H., Migdisov, A. A., Williams-Jones, A. E., van Hinsberg, V. J., Xu, H., and Roback, R., 2021,
The solubility of thorium in carbonate-bearing solutions at hydrothermal conditions:
Geochimica et Cosmochimica Acta

considered in our experiments (log β_4=43.34 and 44.31 at 175 and 200°C, respectively, and log β_5= 46.15 and 47.9 at 225 and 250°C, respectively) to permit forward modeling of Th mobility in natural systems. Our study indicates that carbonate ions are unlikely to play a role in transporting Th in hydrothermal fluids. Summarizing the results of this study and our previous studies of the solubility of Th in hydrothermal fluids, we conclude that SO_4^{2-} is the primary ligand responsible for the hydrothermal transport of Th.

1. Introduction

Thorium, the most abundant actinide in the Earth's crust, is generally considered to be immobile in nature, based on data collected at ambient conditions (Rand et al., 2008). This interpretation, however, is in conflict with observations of hydrothermal Th mineralization, including that of REE ore deposits produced by hydrothermal fluids (Castor, 2008; Sheard et al., 2012; Cook et al., 2013). Owing to its radioactivity, Th is viewed as an unfavorable contaminant, and its enrichment therefore impacts negatively on the feasibility of mining endeavors. There has been growing interest in the past few decades, however, in the possibility of exploiting deposits of Th to substitute for or enhance U nuclear fuels. Consequently, it is necessary to determine the mechanisms responsible for the mobilization, enrichment, and depletion of Th in hydrothermal fluids.

The main impediment to evaluating the transport and deposition of Th by hydrothermal solutions is a lack of information on the behavior and properties of Th-bearing aqueous species at elevated temperature. The published data on this speciation are restricted almost entirely to temperatures below 100°C, with most of the data being for ambient conditions (Rand et al., 2008). We recently launched a research program to address this knowledge gap by conducting solubility experiments involving crystalline ThO_2 at temperatures >175°C in chloride- and sulfate-bearing systems, i.e., systems containing ligands expected to be important in natural hydrothermal systems (Nisbet et al., 2018, 2019). These experiments indicated that SO_4^{2-} has a major impact on the solubility and mobility of Th at elevated temperature (175-250°C),

even if the concentrations of SO_4^{2-} (>0.5m) are modest (Nisbet et al., 2019). A notable gap in our current knowledge is a lack of understanding of the behavior of Th in carbonate-bearing systems. Among the possible complexing ligands, the carbonate anion has been shown to form very stable complexes with actinides, such as Th, at ambient conditions (Rand et al., 2008), and it is logical to speculate, as many researchers have (Wood, 1990; Haas et al., 1995), that this complex may also play a significant role in Th mobility at elevated temperature. Indeed, it is noteworthy that, in nature, thorium tends to concentrate in highly evolved systems that have elevated carbonate concentrations including carbonatites (>50 % carbonate) (Ault et al., 2015). Many of these systems were formed and/or altered by hydrothermal fluids (e.g., Mountain Pass, Bear Lodge; Castor, 2008; Andersen et al., 2017); yet, to date, there have been no investigations of Th solubility and speciation in carbonate-bearing fluids at high temperature. Consequently, the role of carbonate-species in the mobilization of Th in these systems cannot be evaluated.

The thermodynamic data for Th-carbonate speciation have been summarized in a thorough review by the Nuclear Energy Agency (NEA) (Rand et al., 2008). Results of 19 sets of experiments have been reported for aqueous solutions at ambient conditions, all of which show that Th has a strong affinity for carbonate anions. Indeed, reactions involving the complexation of actinides with carbonate have been considered "some of the most important reactions in aqueous systems" (Altmaier et al., 2005). However, there have been serious inconsistencies in the identification of the dominant Th-carbonate species. Altmaier et al. (2005; 2006) identified the ternary complexes $Th(OH)(CO_3)_4^{5-}$ and $Th(OH)_2(CO_3)_2^{2-}$ as the dominant species with minor contributions from $Th(OH)_2(CO_3)_{(aq)}$, $Th(OH)_3(CO_3)^-$ and $Th(OH)_4(CO_3)^{2-}$ in solutions with an ionic strength of 0.5 M. In contrast, Osthols et al. (1994), Felmy et al. (1997) and Felmy and Rai, (1999) proposed that $Th(CO_3)_6^{5-}$ is the dominant complex in solutions containing 0.1-2.0 M CO_3^{2-} and $Th(OH)_3(CO_3)^-$ to dominate at lower carbonate concentrations and near-neutral pH conditions. It should be noted that the above mentioned studies were all conducted using an amorphous ThO_2 reference phase, which has been shown to lead to discrepancies of several orders of magnitude in the measured

concentrations of dissolved Th relative to those using crystalline ThO_2, owing to the higher solubility of amorphous solids (Rand et al., 2008).

Evidently, even at ambient conditions, there is uncertainty regarding Th-carbonate speciation, and at elevated temperature, thermodynamic data are simply non-existent. The purpose of this study is to investigate the speciation of Th in carbonate-bearing fluids at hydrothermal conditions and to derive the thermodynamic properties of the dominant complexes to permit forward modeling of Th mobility in natural, carbonate-bearing hydrothermal systems.

2. Methods

To investigate the speciation of Th in carbonate-bearing solutions, solubility experiments were performed in solutions of varying carbonate concentration (0.05-0.5m $NaHCO_3/Na_2CO_3$, pH_T 7.83-9.82) at elevated temperature (175-250°C) and the pressure of saturated water vapor, with crystalline thorium dioxide (ThO_2) as the solid reactant (particle size >10 μm). The experimental solutions were contained in Teflon-lined titanium autoclaves. Before each experiment, small Teflon tubes containing crystalline ThO_2 (IBI Labs, Technical Grade 99.8%), capped with a porous Teflon film, were placed in the Teflon reactors and submerged in 10 mL of solution. The autoclaves were then sealed with a Teflon O-ring, and placed in a Muffle Furnace for 12-14 days. At the end of an experiment, the autoclaves were removed from the furnace and immediately quenched in a stream of cold air (the quench time was < 25min). The Teflon tubes were removed as soon as the solutions were quenched. The addition of the Teflon film ensured that the exchange between the ThO_2 and the experimental solution was slowed down such that the measured solubility was not altered during quenching and heating. Considering that equilibrium with the solution was reached within 3 days (see below) and quenching and heating takes less than 25 min, we consider the concentrations measured in the quenched aqueous solutions to correspond to isothermal solubility. A 3mL aliquot of sulfuric acid (Fisher Scientific, TraceMetal Grade) was then added to the solutions and left for

24 hours to dissolve any Th that may have precipitated on the walls of the reactor. Finally, Th concentrations in the resulting solutions were measured via Inductively Coupled Plasma Mass Spectrometry (ICP-MS) at the Geochemical and Geomaterials Research Laboratories of the Los Alamos National Laboratory. A sketch of the experimental setup is shown in Figure 1.

Two sets of experimental solutions were prepared to determine the solubility of Th as a function of carbonate activity: 1) solutions containing 0.05-0.5 m $NaHCO_3$ and 2) solutions containing 0.05-0.5 m Na_2CO_3, each with a constant 1 m concentration of NaCl. The pH of the experimental solutions was calculated based on the concentrations of $NaHCO_3$ and Na_2CO_3 added, as described below. The presence of NaCl in the experimental solutions was required to satisfy the activity model used in our calculations. Targeted amounts of $NaHCO_3$ (Acros Organics, A.C.S. grade), Na_2CO_3(anhydrous, Fisher Chemical, A.C.S. grade), and NaCl (Fisher Chemical, A.C.S. grade) were added to vacuum-degassed deionized water (DI) that was flushed with argon gas immediately before sealing of the autoclaves to minimize the exchange of CO_2 between the fluid and the atmosphere. Parameters for each experiment are reported in Table 1.

To prevent contamination between experiments, the Teflon reactors and titanium autoclaves were soaked in a 5% nitric acid solution (Fisher Chemical, TraceMetal Grade) prepared with deionized water. A series of washing solutions were analyzed alongside the experimental solutions to verify there was no residual Th in the vessels. The time required to reach a steady-state concentration was determined through a time series of experiments, in which autoclaves containing solutions of identical composition (0.25m $NaHCO_3$) were heated at 175°C and removed sequentially over 14 days (Table 2). A steady-state concentration was reached within 3 days; the time would be less at higher temperature because of a higher rate of reaction. All the experiments had a minimum duration of 12 days. As in our previous experiments (Nisbet et al., 2018; 2019), the solid reactant (crystalline ThO_2) was analyzed by X-Ray Diffraction (XRD) to ensure that no new phases formed during the experiments, and that the solubility measured corresponded to saturation of the fluid with respect to this phase.

3. Results and data treatment

The results of the solubility experiments are reported in Table 1. This table lists the concentration of $NaHCO_3$ and Na_2CO_3 in the solution added to each autoclave, the logarithm of the concentration of Th measured in the solutions after each experiment, the calculated activity of HCO_3^- and the pH calculated for the experimental temperature (pH_T). In order to determine the pH_T and the activity of HCO_3^-, we used the thermodynamic modeling software, HCh (Shvarov and Bastrakov, 1999). The model that was employed included the following species: H_2O, H^+, OH^-, O_2, H_2, Na^+, NaOH°, NaCl°, Cl^-, HCl°, CO, CO_2, CO_3^{2-}, HCO_3^-, $NaCO_3^-$, $NaHCO_{3(aq)}$, $NaHCO_{3(s)}$ $Na_2CO_{3(s)}$, with thermodynamic data taken from Johnson et al. (1992), Shock et al. (1997), Sverjensky et al. (1997), and Tagirov et al. (1997). Aqueous Th species were not included in these initial calculations as it was assumed that the low concentration of Th dissolved in the solution did not make a significant contribution to the pH of the solution. The thermodynamic properties of water and its dissociation constant were calculated using the Haar-Gallagher-Kell model (Kestin et al., 1984) and the Marshall and Franck model (Marshall and Franck, 1981), respectively. To date, the most reliable and accurate high-T thermodynamic calculations are those performed in NaCl-dominant solutions. This limitation is due to the relative paucity of activity models tuned and experimentally verified at elevated temperature for other background electrolytes. The need for an experimentally proven activity model is why all the experiments were designed to be NaCl-dominant. The model used in these, and all subsequent calculations was the extended Debye-Hückel model modified by Helgeson et al. (1981), Oelkers and Helgeson (1990), and Oelkers and Helgeson (1991), which is recommended for NaCl-dominated solutions up to an ionic strength of 6, and a temperature up to 600°C:

$$\log \gamma_i = -\frac{AZ_i^2\sqrt{I}}{1+B\dot{a}\sqrt{I}} + b_\gamma I + \Gamma \quad (1)$$

where A and B are the Debye-Hückel solvent parameters, γ_i, Z_i and $\dot{a}_\iota$ are the individual molal activity coefficient, the charge, and the distance of closest approach of an ion i, respectively. The effective ionic strength calculated using the molal scale is I, Γ is a molarity to molality conversion factor, $\Gamma =$

$-log_{10}(1 + 0.0180153m_{\Sigma})$, where m_{Σ} is the sum of molalities of all dissolved species, and b_{γ} is the extended-term parameter for NaCl from Helgeson et al. (1981). Using this model, the pH_T and the $aHCO_3^-$ was calculated for each experimental temperature. The solution compositions fixed the pH_T range between 7.8 and 9.8 for each temperature.

3.1 Determination of predominant aqueous species

Irrespective of whether $NaHCO_3$ or Na_2CO_3 was added to the solution, each of the experiments was conducted in the predominance field of HCO_3^- (Fig. 2). It should be noted that, although conditions our experiments do not fall within the predominance field of CO_3^{2-}, such conditions are also very unlikely to occur in natural hydrothermal systems. Considering that the pK of water is 11.4 at 175°C and 11.2 at 250°C, the condition of neutrality at these temperatures corresponds to pH_T values of 5.7 and 5.6, respectively. Therefore, the conditions tested in our experiments (pH_T 7.8-9.8) were extremely alkaline. Moreover, it has been shown that the formation constant of $An(HCO_3)^+$ for trivalent actinides is 4-5 orders of magnitude lower than that of $An(CO_3)^+$at ambient conditions (Ciavatta et al., 1981; Spahiu, 1985; Guillaumont and Mompean, 2003) and it is expected that the difference will be even larger for the formation of tetravalent metal ion bicarbonate complexes, such as those of Th (Rand et al. 2008). Therefore, to evaluate whether Th-carbonate species predominate in solution, the logarithm of the concentration of Th was plotted as a function of the activity of HCO_3^- for both sets of experiments (Figs. 3-4). As shown in Figures 3 and 4, the concentration of Th is independent of the activity of HCO_3^- over the entire temperature range, and for each set of experiments.

The lack of dependence of the measured Th concentration on the activity of carbonate indicates that Th-carbonate complexes were not present in detectable concentrations at the conditions investigated in our experiments. Moreover, although Cl^- is an important ligand in the experimental system and, in principle, could form stable complexes with Th, Th-chloride complexes have not been detected in previous

experiments at comparable experimental conditions (Nisbet et al., 2018). This suggests, as in the experiments of Nisbet et al. (2018), that Th-hydroxyl complexes predominated in the experiments conducted in the current study. We tested this hypothesis by analyzing the pH_T dependency of the saturation concentration of Th in our experimental solutions, each of which had a specific pH_T that depended on the molality of $NaHCO_3$ or Na_2CO_3 in the starting solutions. In order to determine if Th-hydroxyl complexes did, indeed, predominate at the experimental conditions, the logarithm of the measured concentrations of Th for the sets of experiments were plotted as a function of the pH_T at each temperature (Fig. 5).

As shown in the plots presented in Figure 5, the concentration of Th defines two trends: 1) at the lower experimental temperatures (175 and 200°C), the concentration of Th is nearly independent of pH_T (it decreases slightly with increasing pH_T and 2) at the higher temperatures (225 and 250°C), it increases linearly with pH_T at a slope of approximately +1 (0.71 and 0.91). This suggests that the dominant Th-hydroxyl species in solution are $Th(OH)_4^0$ and $Th(OH)_5^-$ at the lower and higher temperatures, respectively, and that they formed via the reactions:

$$ThO_2 + 2H_2O \leftrightarrow Th(OH)_4^0 \quad (2)$$

$$ThO_2 + 3H_2O \leftrightarrow Th(OH)_5^- + H^+. \quad (3)$$

An additional set of experiments was performed at 250°C, using solutions containing a mixture of $NaHCO_3$ and Na_2CO_3 (0.05-0.5m), to establish an intermediate pH and better constrain the trend in the data.

Although the slopes observed in these figures deviate a little from the stoichiometric slope suggested by Reactions 2 and 3, due possibly to a change in the activity of the Th species, it needs to be emphasized that this graphical analysis is a preliminary, semi-quantitative step designed to determine the probable stoichiometry of the species. Reliable determination of the stoichiometry of the predominant species and evaluation of their stability require a more complex numerical fitting that accounts for all the factors

influencing the concentration of Th in the experimental solutions. This fitting is reported in the following section.

3.2 Derivation of formation constants

The experimental data reported in Table 1 were used to confirm the stoichiometry of the predominant species interpreted from the simple graphical analysis discussed above, and to calculate thermodynamic formation constants for these species. As discussed below, these species were confirmed to be $Th(OH)_4^0$ and $Th(OH)_5^-$, for which the corresponding formation reactions are:

$$Th^{4+} + 4OH^- \leftrightarrow Th(OH)_4^0 \quad (4)$$

$$\log \beta_4 = \log a_{Th(OH)_4^0} - \log a_{Th^{4+}} - 4 \log a_{OH^-} \quad (5)$$

and

$$Th^{4+} + 5OH^- \leftrightarrow Th(OH)_5^- \quad (6)$$

$$\log \beta_5 = \log a_{Th(OH)_5^-} - \log a_{Th^{4+}} - 5 \log a_{OH^-}. \quad (7)$$

In our earlier study (Nisbet et al., 2018), we reported thermodynamic formation constants for $Th(OH)_4^0$ from solubility experiments conducted in chloride-bearing solutions under acidic conditions (pH_T ~1.7-4.0). However, it should be noted that, owing to the experimental conditions, these constants were based on limited data. Thus, in this contribution, we have combined the data from the current set of experiments in which our graphical analysis predicted that $Th(OH)_4^0$ is the dominant complex (175 and 200°C), with the data from our previous experiments (Nisbet et al., 2018) to better constrain the thermodynamic parameters and extract more reliable stability constants. The calculations were performed using the program, OptimA, which is part of the HCh software package (Shvarov and Bastrakov, 1999). OptimA iteratively derives the standard Gibbs free energies of formation of aqueous species by minimizing the sum of the squared deviations of the experimental concentrations for the species of interest from their

concentrations calculated using the equilibrium composition of the solution in all experiments at the relevant P-T conditions (Shvarov, 2015). In addition to the species specified in the model described above, the model also included the following species: $ThO_{2(s)}$, Th^{4+}, $Th(OH)_2^{2+}$, and $Th(OH)_4^0$. Data for $ThO_{2(s)}$ and Th^{4+} were taken from Robie and Hemingway (1995) and Shock et al. (1997), respectively, data for $Th(OH)_2^{2+}$ and $Th(OH)_4^0$ were taken from Nisbet et al. (2018) ; the stability parameters of $Th(OH)_4^0$ and $Th(OH)_5^-$ were adjustable. Considering that we did not observe any dependency of the solubility of ThO_2 on the carbonate concentration in the experimental solutions, Th-carbonate species were deemed insignificant to the mass balance of dissolved Th and were not included in the model. Likewise, as Nisbet et al. (2018), did not detect Th-chloride species in their experiments, these species were also not accounted for in the model. It should be noted that the contribution of polynuclear species to the solubility of Th was also not considered in our model, as it can be assumed that these species become unstable at high temperatures due to the decrease in the dielectric constant of water and the associated increase in electrostatic repulsion at elevated temperature (Brugger et al., 2014; Seward et al., 2014). This is further supported by previous analyses conducted using Extended X-Ray Absorption Fine Structure (EXAFS), which found no evidence for the formation of polynuclear species in bicarbonate and carbonate solutions at concentrations above 0.1 M at ambient conditions (Felmy et al., 1997; Altmaier et al., 2006). The resulting formation constants for $Th(OH)_4^0$ and $Th(OH)_5^-$ derived for their respective experimental temperatures are reported in Table 3, together with their uncertainties.

3.3. Derivation of MRB parameters

The revised thermodynamic formation constants for $Th(OH)_4^0$ derived in this study for 175°C and 200°C are an average of 1.1 log units higher than those published in Nisbet et al. (2018). This is not surprising considering that the values reported in Nisbet et al. (2018) for these temperatures were derived from only a few experimental data points. To refine these values, the new thermodynamic formation constants were combined with our previous values for 225 and 250°C (43.17 and 43.74, respectively), in a fit to the Ryzhenko-Bryzgalin model (MRB) (Ryzhenko et al., 1985), modified by Borisov and Shvarov (1992) as

described in Shvarov and Bastrakov (1999). This allowed us to interpolate the data and also extrapolate them to ambient temperature for comparison to previously reported formation constants for 25°C. The MRB model fits the temperature and pressure dependence of the dissociation constant for ion pairs through the following equation:

$$logK_{(T,P)} = \frac{T_r}{T} logK_{(T_r,P_r)} + B_{(T,P)}(A_{zz/a} + \frac{B_{zz/a}}{T}) \quad (8)$$

where K is the dissociation constant of the ion pair, T_r and P_r are the reference temperature and pressure, respectively, $B_{(T,P)}$ accounts for the property of water at the temperature and pressure calculated from the data in Marshall and Franck (1981), and $A_{zz/a}$ and $B_{zz/a}$ are the fitting parameters. The revised MRB parameters for $Th(OH)_4^0$ are reported in Table 4, and Figure 6 shows the results of the optimization as well as data previously reported for ambient conditions (Baes Jr. et al., 1965; Baes and Mesmer, 1976; Moon, 1989; Grenthe and Lagerman, 1991; Moriyama et al., 1999; Ekberg et al., 2000; Neck and Kim, 2001). As can be seen from Figure 6, the revised log β values are consistent with those published for 25°C. However, given the high degree of extrapolation required, the reliability of the fit at 25°C is lower than that interpolated within the experimental temperature range.

Thermodynamic formation constants were derived for $Th(OH)_5^-$ at 225 and 250°C. To the best of our knowledge, the only study that has reported the presence of $Th(OH)_5^-$ in an aqueous solution is that of Gayer and Leider (1954), who conducted solubility experiments with $ThO(OH)_2$(s) in $HClO_4$ and NaOH solutions at 25°C. The equilibrium constant presented in this study, however, was considered unreliable in a subsequent review of the chemical thermodynamics of thorium because the study did not involve filtration or centrifugation steps following the experiments and, therefore, may have overestimated the concentration of Th due to the presence of colloids (Rand et al., 2008). The absence of a reliable formation constant for $Th(OH)_5^-$ at ambient conditions makes it challenging to extrapolate our high temperature formation constants for this species to 25 °C with any confidence. In order to try and overcome this limitation, we estimated the thermodynamic formation constant for $Th(OH)_5^-$ at 25°C from

the change in the stability of Th-hydroxyl species with the degree of hydrolysis, using log β values reported for 25°C in Neck and Kim (2001) for $Th(OH)^{3+}$ and $Th(OH)_3^+$, for $Th(OH)_2^{2+}$ in Nisbet et al. (2018) and for $Th(OH)_4^0$ (this study). The polynomial fit of these data is shown in Figure 7, together with the estimated value for $Th(OH)_5^-$. Using this log β at 25°C and the experimentally derived values at 225 and 250°C, the data were interpolated using the MRB model, as described above (Fig. 8). A set of MRB parameters were derived for $Th(OH)_5^-$ and are reported in Table 5.

4. Th speciation in natural hydrothermal fluids

The relative proportions of the various Th-hydroxyl species as a function of pH at the temperature of our experiments is illustrated in Figure 9. As is evident from this figure, there is a progressive shift in the predominance of the complexes from $Th(OH)_2^{2+}$ at low pH to $Th(OH)_4^0$ and $Th(OH)_5^-$ at high pH. This increase in the degree of the hydrolysis of ThO_2 with increasing pH is a predictable consequence of the increase in the concentration of OH^- ions available for complexation with Th^{4+} in the solution. The most notable change with temperature is the shift in the predominance of $Th(OH)_5^-$ to lower pH as temperature increases and a related decrease in the size of the $Th(OH)_4^0$ predominance field.

Hard Soft Acid Base (HSAB) theory (Pearson, 1963) predicts that strong acids, such as the Th^{4+} ion, will preferentially react and form stable complexes with strong bases. In general, strong bases are ligands that have low polarizability, a small ionic radius, and a high oxidation state (Pearson, 1963), and these include the anions CO_3^{2-} and SO_4^{2-} that are abundant in nature. Our previous experiments on Th speciation in sulfate-bearing fluids at elevated temperature demonstrated that Th has a very high affinity for SO_4^{2-}, with the stable $Th(SO_4)_2$ complex predominating over the entire temperature range (175-250°C; Nisbet et al., 2019). In contrast, the data reported in this study indicate that aqueous Th-carbonate complexes do not predominate at temperatures >175°C. Instead, the solubility of ThO_2 is governed by hydrolysis reactions and the species $Th(OH)_4^0$ and $Th(OH)_5^-$. The failure to detect the formation of Th-carbonate complexes at elevated temperature is in stark contrast to the results of studies conducted at ambient conditions, which

showed that carbonate ions form strong complexes with Th. Irrespective of the reason for the sharp decrease in the stability of Th-carbonate complexes at elevated temperature, the essential finding of our experiments is that carbonate-bearing solutions are unlikely to transport Th in hydrothermal systems. To identify the species that may be responsible for the transport of Th in hydrothermal fluids, we constructed diagrams showing the predominance of various Th complexes at 200 and 250°C as a function of pH_T and the logarithm of the activity of SO_4^{2-} (Fig. 10). The diagrams shown in this figure consider all the Th species for which there are currently high T data: Th^{4+}, $Th(OH)_2^{2+}$, $Th(OH)_4^0$, $Th(OH)_5^-$ and $Th(SO_4)_2$. Under acidic conditions, $Th(OH)_2^{2+}$ is predicted to dominate only when the sulfate concentration is extremely low. In the presence of even minor sulfate, $Th(SO_4)_2$ is predicted to be more stable. Concentrations of sulfate in hydrothermal solutions frequently go unreported, and where mentioned are commonly based on the presence of minerals such as anhydrite and gypsum. Some authors, however, have reported concentrations of sulfate from fluid inclusion studies, primarily from REE-bearing hydrothermal fluids; these fluids are relevant to Th transport as these systems have been shown to have higher than average Th concentrations due to the similar ionic radii and charges of Th and the REE. These authors have reported concentrations of sulfate that range from 0.2-2.5m (Banks et al., 1994; Williams-Jones et al., 2000) which, based on the predominance diagrams (Fig. 10), indicates that Th will be transported as a sulfate complex under acidic to moderately acidic conditions (modeled in Nisbet et al.. 2019). As pH increases to neutral and alkaline conditions, the speciation of Th is dominated by the Th-hydroxyl species, $Th(OH)_4^0$ and $Th(OH)_5^-$. Under these conditions, the concentration of Th in solution is expected to be low, owing to the relatively low stability of these complexes. Therefore, given the data available to date for Th speciation at elevated temperature, we predict that the $Th(SO_4)_2^0$ complex is one of the major vehicles for the transport of Th, that Th-hydroxyl species play a minor role in this transport, and that carbonate species are insignificant.

5. Conclusion

The experimental data collected in this study demonstrate that there is negligible Th-carbonate complexation at elevated temperature (>175°C) in carbonate-bearing solutions (0.05-0.5m $NaHCO_3/Na_2CO_3$). This result is in sharp contrast to the results of experiments performed at ambient conditions for which Th-carbonate species are reported to be highly stable. Instead, hydrolysis of Th is the major control on the solubility of ThO_2, with $Th(OH)_4^0$ predominating at 175 and 200°C and $Th(OH)_5^-$ at 225 and 250°C. Thermodynamic formation constants were derived for these complexes at their respective temperatures. Based on the data currently available for Th complexation at elevated temperature, our results indicate that carbonate is unlikely to play a role in the transport of Th in natural hydrothermal systems, and that $Th(SO_4)_2^0$ complex is the main species controlling the mobilization of Th.

Acknowledgments

We would like to thank Joshua White for conducting the XRD analyses, and Oana Marina and Chelsea Neil for performing the ICP-MS analyses.

Funding: This work was supported by the Laboratory Directed Research and Development (LDRD) program of Los Alamos National Laboratory (LANL), New Mexico, USA (project number 20180007DR), and by LANL's Center for Space and Earth Sciences (CSES). CSES is funded by LANL's LDRD program under project number 20180475DR.

References

Altmaier M., Neck V., Denecke M. A., Yin R. and Fanghänel T. (2006) Solubility of ThO2·xH2O(am) and the formation of ternary Th(IV) hydroxide-carbonate complexes in NaHCO3-Na2CO3 solutions containing 0−4 M NaCl. *Radiochimica Acta* **94**.

Altmaier M., Neck V., Müller R. and Fanghänel T. (2005) Solubility of ThO2·xH2O(am) in carbonate solution and the formation of ternary Th(IV) hydroxide-carbonate complexes. *Radiochimica Acta* **93**.

Andersen A. K., Clark J. G., Larson P. B. and Donovan J. J. (2017) REE fractionation, mineral speciation, and supergene enrichment of the Bear Lodge carbonatites, Wyoming, USA. *Ore Geology Reviews* **89**, 780–807.

Ault T., Van Gosen B., Krahn S. and Croff A. (2015) Natural thorium resources and recovery: options and impacts. *Nuclear Technology* **194**, 136–151.

Baes C. F. and Mesmer R. S. (1976) The hydrolysis of cations. *Ber. Bunsenges. Phys. Chem.* **81**, 245–246.

Baes Jr. C. F., Meyer N. J. and Roberts C. E. (1965) The Hydrolysis of Thorium(1V) at 0 and 95°C. *Inorganic Chemistry* **4**, 518–527.

Banks D. A., Yardley B. W. D., Campbell A. R. and Jarvis K. E. (1994) REE composition of an aqueous magmatic fluid: A fluid inclusion study from the Capitan Pluton, New Mexico, U.S.A. *Chemical Geology* **113**, 259–272.

Borisov M. V. and Shvarov Y. V. (1992) Thermodynamics of geochemical processes. *Moscow, Moscow State University Publishing House*, 254.

Brugger J., Tooth B., Etschmann B., Liu W., Testemale D., Hazemann J.-L. and Grundler P. V. (2014) Structure and Thermal Stability of Bi(III) Oxy-Clusters in Aqueous Solutions. *Journal of Solution Chemistry* **43**, 314–325.

Castor S. B. (2008) The Mountain Pass rare-earth carbonatite and associated ultrapotassic rocks, California. *The Canadian Mineralogist* **46**, 779–806.

Ciavatta L., Ferri D., Grenthe I., Salvatore F. and Spahiu K. (1981) Studies on Metal Carbonate Equilibria. 3. The Lanthanum(III) Carbonate Complexes in Aqueous Perchlorate Media. *Acta Chem. Scand.* **35a**, 403–413.

Cook N. J., Ciobanu C. L., O'Rielly D., Wilson R., Das K. and Wade B. (2013) Mineral chemistry of Rare Earth Element (REE) mineralization, Browns Ranges, Western Australia. *Lithos* **172–173**, 192–213.

Ekberg C., Albinsson Y., Comarmond M. J. and Brown P. L. (2000) Study on the complexation behavior of thorium(IV).1. Hydrolysis equilibria. *Journal of Solution Chemistry* **29**, 63–86.

Felmy A. R. and Rai D. (1999) Application of Pitzer's Equations for Modeling the Aqueous Thermodynamics of Actinide Species in Natural Waters: A Review. *Journal of Solution Chemistry* **28**, 533–553.

Felmy A. R., Rai D., Sterner S. M., Mason M. J., Hess N. J. and Conradson S. D. (1997) Thermodynamic models for highly charged aqueous species: Solubility of Th(IV) hydrous oxide in concentrated NaHCO3 and Na2CO3 solutions. *Journal of Solution Chemistry* **26**, 233–248.

Gayer K. H. and Leider H. (1954) The Solubility of Thorium Hydroxide in Solutions of Sodium Hydroxide and Perchloric Acid at 25°C. *J. Am. Chem. Soc.* **76**, 5938–5940.

Grenthe I. and Lagerman B. (1991) Studies on metal carbonate equilibria: 23. Complex formation in the Th(IV)-H2O-CO2(g) system. *Acta Chemica Scandinavica* **45**, 231–238.

Guillaumont R. and Mompean F. J. (2003) *UPDATE ON THE CHEMICAL THERMODYNAMICS OF URANIUM, NEPTUNIUM, PLUTONIUM, AMERICIUM AND TECHNETIUM*., Elsevier.

Haas J. R., Shock E. L. and Sassani D. C. (1995) Rare earth elements in hydrothermal systems: Estimates of standard partial molal thermodynamic properties of aqueous complexes of the rare earth elements at high pressures and temperatures. *Geochimica et Cosmochimica Acta* **59**, 4329–4350.

Helgeson H. C., Kirkham D. H. and Flowers G. C. (1981) Theoretical prediction of the thermodynamic behavior of aqueous electrolytes at high pressures and temperatures: IV. Calculation of activity coefficients, osmotic coefficients, and apparent molal and standard and relative partial molal properties to 600°C. *American Journal of Science* **281**, 1249–1516.

Johnson J. W., Oelkers E. H. and Helgeson H. C. (1992) SUPCRT92: a software package for calculating the standard molal thermodynamic properties of minerals, gases, aqueous species, and reactions from 1 to 5000 bar and 0 to 1000 °C. *Computational Geosciences* **18**, 899–947.

Kestin J., Sengers J. V., Kamgar-Parsi B. and Levelt Sengers J. M. H. (1984) Thermophysical properties of fluid H2O. *Journal of Physical and Chemical Reference Data* **13**, 601–609.

Marshall W. L. and Franck E. U. (1981) Ion product of water substance, 0-1000 °C, 1-10,000 bars new International Formulation and its background. *Journal of Physical and Chemical Reference Data* **10**, 295–304.

Moon H. (1989) Equilibrium ultrafiltration of hydrolyzed thorium(IV) solutions. *Bulletin of the Korean Chemical Society* **10**, 270–272.

Moriyama H., Kitamura A., Fujiwara K. and Yamana H. (1999) Analysis of mononuclear hydrolysis constants of actinide ions by hard sphere model. *Radiochimica Acta* **87**, 97–104.

Neck V. and Kim J. I. (2001) Solubility and hydrolysis of tetravalent actinides. *Radiochimica Acta* **89**, 1–16.

Nisbet H., Migdisov A. A., Williams-Jones A. E., Xu H., van Hinsberg V. J. and Roback R. (2019) Challenging the thorium-immobility paradigm. *Sci Rep* **9**, 17035.

Nisbet H., Migdisov A., Xu H., Guo X., van Hinsberg V., Williams-Jones A. E., Boukhalfa H. and Roback R. (2018) An experimental study of the solubility and speciation of thorium in chloride-bearing aqueous solutions at temperatures up to 250 °C. *Geochimica et Cosmochimica Acta* **239**, 363–373.

Oelkers E. H. and Helgeson H. C. (1991) Calculation of activity coefficients and degrees of formation of neutral ion pairs in supercritical electrolyte solutions. *Geochimica et Cosmochimica Acta* **55**, 1235–1251.

Oelkers E. H. and Helgeson H. C. (1990) Triple-ion anions and polynuclear complexing in supercritical electrolyte solutions. *Geochimica et Cosmochimica Acta* **54**, 727–738.

Osthols E., Bruno J. and Grenthe I. (1994) On the influence of carbonate on mineral dissolution: III. The solubility of microcrystalline ThO2 in CO2-H2O media. *Geochimica et Cosmochimica Acta* **58**, 613–623.

Pearson R. G. (1963) Hard and soft acids and bases. *Journal of the American Chemical Society* **85**, 3533–3539.

Rand M. H., Mompean F. J., Perrone J. and Illemassene M. (2008) *Chemical Thermodynamics of Thorium*., OECD, NEA.

Robie R. A. and Hemingway B. S. (1995) Thermodynamic properties of minerals and related substances at 298.15 K and 1 Bar (10^5 Pascals) pressure and at higher temperatures. *U.S. Geological Survet Bulletin* **2131**, 461.

Ryzhenko B. N., Bryzgalin O. V., Artamkina I. Y., Spasennykh M. Y. and Shapkin A. I. (1985) An electrostatic model for the electrolytic dissociation of inorganic substances dissolved in water. *Geochemistry International* **22**, 138–144.

Seward T. M., Williams-Jones A. E. and Migdisov A. A. (2014) The Chemistry of Metal Transport and Deposition by Ore-Forming Hydrothermal Fluids. In *Treatise on Geochemistry* Elsevier. pp. 29–57.

Sheard E. R., Williams-Jones A. E., Heiligmann M., Pederson C. and Trueman D. L. (2012) Controls on the Concentration of Zirconium, Niobium, and the Rare Earth Elements in the Thor Lake Rare Metal Deposit, Northwest Territories, Canada. *Economic Geology* **107**, 81–104.

Shock E. L., Sassani D. C., Willis M. and Sverjensky D. A. (1997) Inorganic species in geological fluids: Correlations among standard molal thermodynamic properties of aqueous ions and hydroxide complexes. *Geochimica et Cosmochimica Acta* **61**, 907–950.

Shvarov Y. V. (2015) A suite of programs, OptimA, OptimB, OptimC, and OptimS compatible with the Unitherm database, for deriving the thermodynamic properties of aqueous species from solubility, potentiometry and spectroscopy measurements. *Applied Geochemistry* **55**, 17–27.

Shvarov Y. V. and Bastrakov E. (1999) HCh, A Software Package for Geochemical Equilibrium Modeling: User's Guide.

Spahiu K. (1985) Studies on metal carbonate equilibria. XI: Yttrium (III) carbonate complex formation in aqueous perchlorate media of various ionic strengths. *Acta chemica Scandinavica* **A39**, 33–45.

Sverjensky D. A., Shock E. L. and Helgeson H. C. (1997) Prediction of the thermodynamic properties of aqueous metal complexes to 1000 °C and 5 kb. *Geochimica et Cosmochimica Acta* **61**, 1359–1412.

Tagirov B. R., Zotov A. and Akinfiev N. (1997) Experimental study of dissociation of HCl from 350 to 500 °C and from 500 to 2500 bars: thermodynamic properties of HCl°(aq). *Geochimica et Cosmochimica Acta* **61**, 4267–4280.

Williams-Jones A. E., Samson I. M. and Olivo G. R. (2000) The Genesis of Hydrothermal Fluorite-REE Deposits in the Gallinas Mountains, New Mexico. *Economic Geology* **95**, 327–342.

Wood S. A. (1990) The aqueous geochemistry of the rare-earth elements and yttrium 2. Theoretical predictions of speciation in hydrothermal solutions to 350°C at saturation water vapor pressure. *Chemical Geology* **88**, 99–125.

Figures

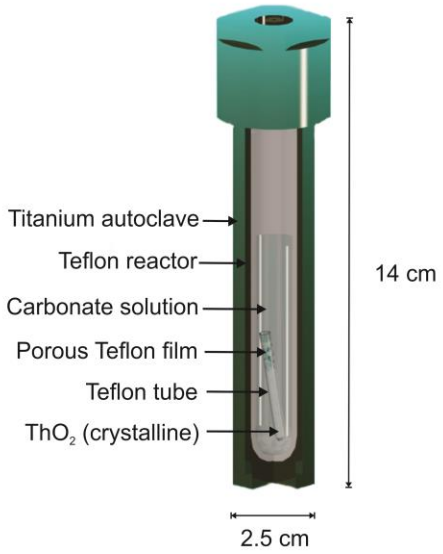

Figure 1. Sketch showing the autoclave set-up used in the experiments.

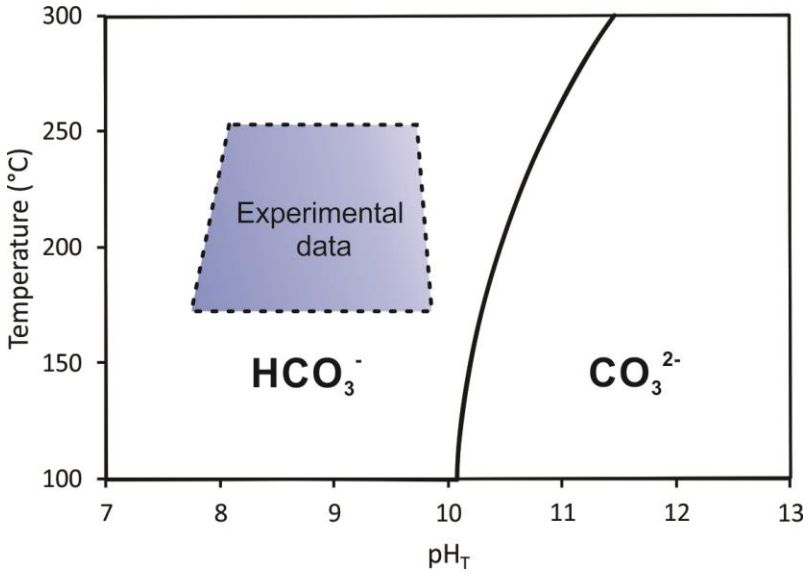

Figure 2. Carbonate predominance diagram with respect to temperature and pH, calculated based on activity using the data of Johnson et al. (1992). The blue area corresponds to the field of our experimental data, demonstrating that all the experiments were conducted in the predominance field of HCO_3^-.

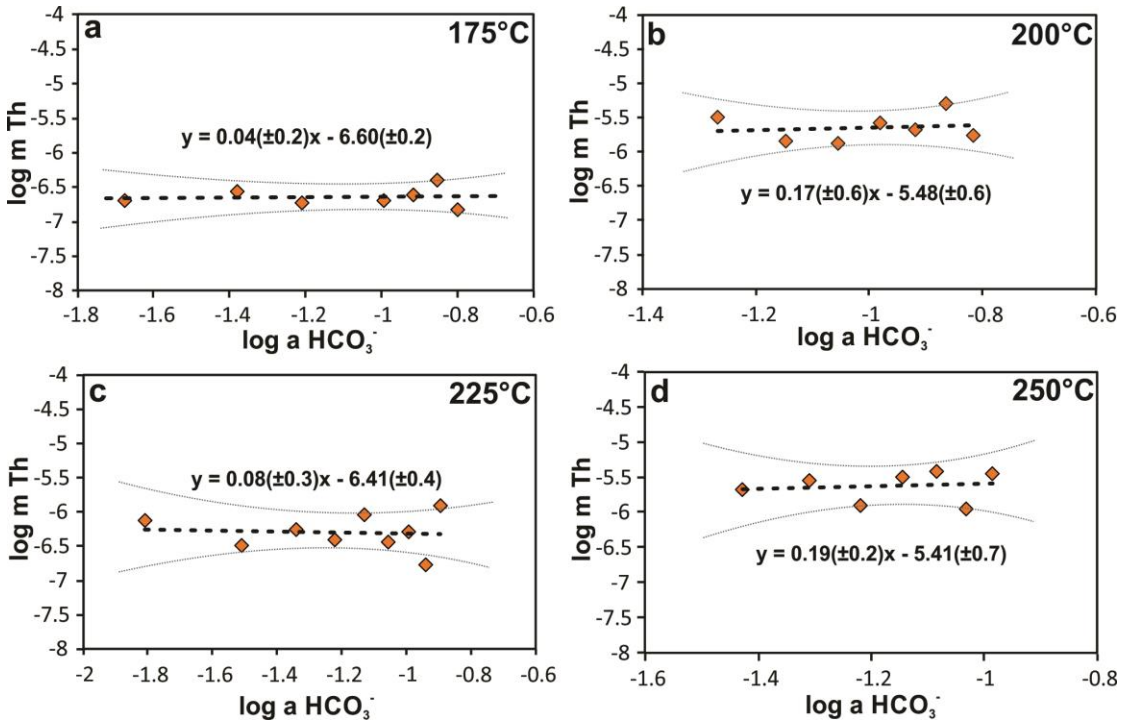

Figure 3a-d. The solubility of Th in $NaHCO_3$ solutions, plotted as a function of the logarithm of the activity of HCO_3^- at (a)175°C, (b) 200°C, (c) 225°C, and (d) 250°C. Each data point represents the logarithm of the concentration of Th (in molality) measured in each autoclave. The trend lines represent a

linear least-squares fit of the data and are accompanied by an error envelope of 95% confidence. In all plots, the slope is not significantly different from 0.

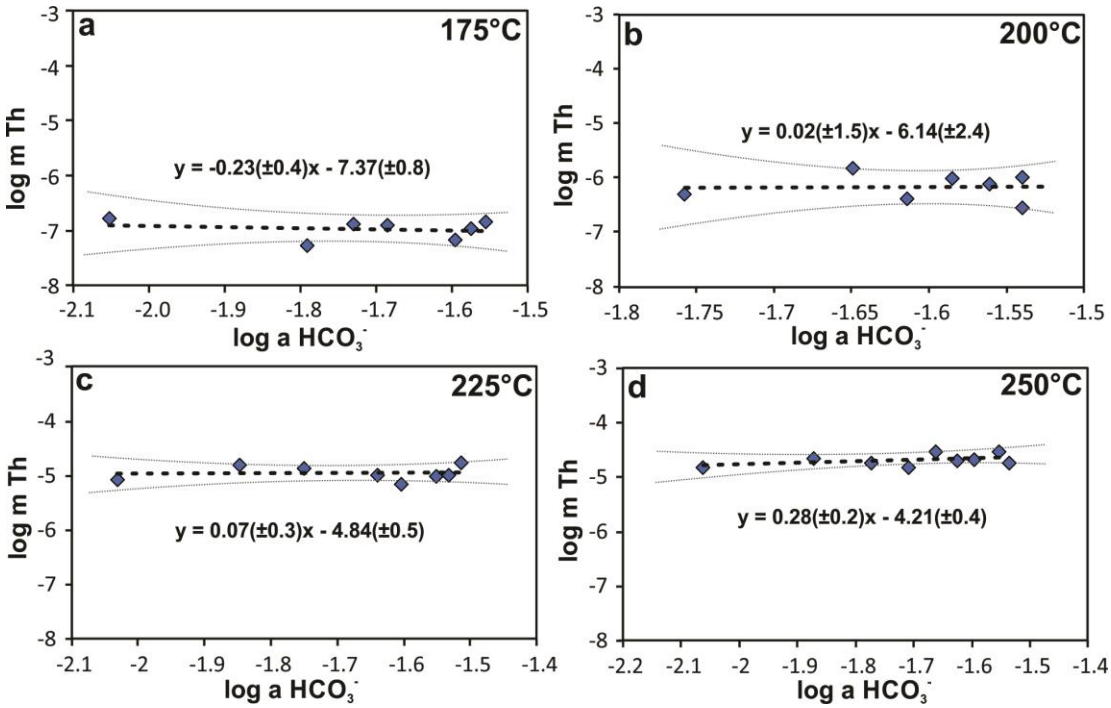

Figure 4a-d. The solubility of Th in Na_2CO_3 solutions, plotted as a function of the logarithm of activity of HCO_3^- at (a) 175°C, (b) 200°C, (c) 225°C, and (d) 250°C. Each data point represents the logarithm of the concentration of Th (in molality) measured in each autoclave. The trend lines represent the linear least-squares fit of the data and are accompanied by an error envelope of 95% confidence. In all plots, the slope is not significantly different from 0.

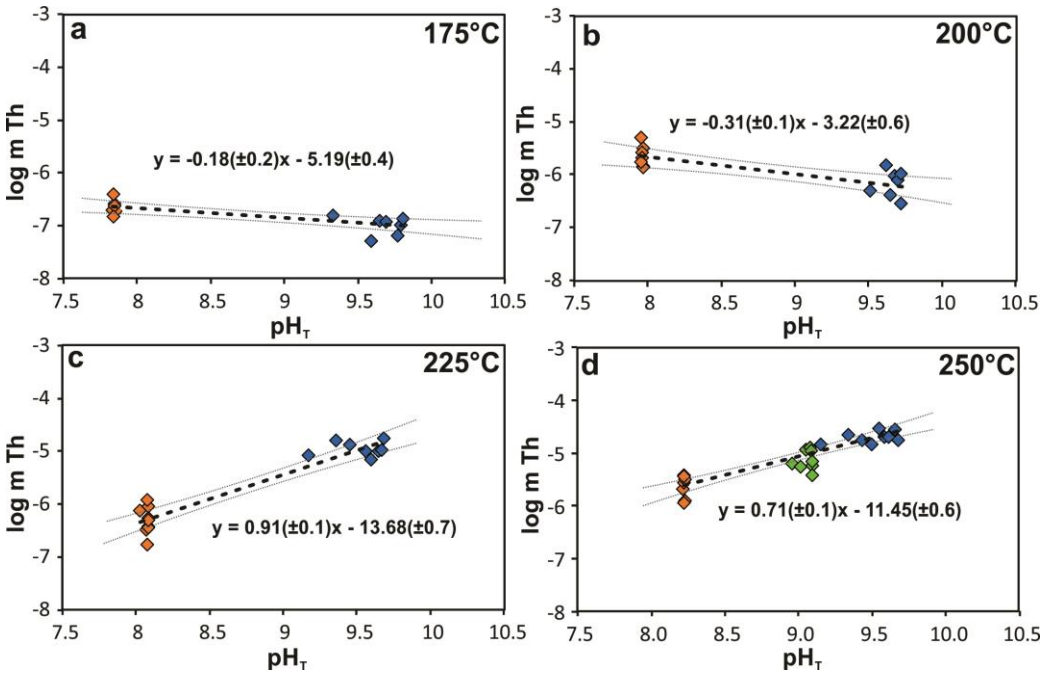

Figure 5a-d. The solubility of Th in $NaHCO_3$ and Na_2CO_3 solutions as a function of the pH at the experimental temperature (a) 175°C, (b) 200°C, (c) 225°C, and (d) 250°C. The slope of the linear leas-squares fit to the data (dashed lines) provides a preliminary indication of the dominant Th hydroxyl species in solution. The small change in the concentration of Th with pH_T in plots a and b suggests an independence of pH (slope ~0), and the predominance of $Th(OH)_4^{0.}$ In contrast, the slope of the data in plots c and d is ~1, suggesting that $Th(OH)_5^-$ was predominant. An error envelope of the fit at 95% confidence is shown by the fine dotted lines in each plot.

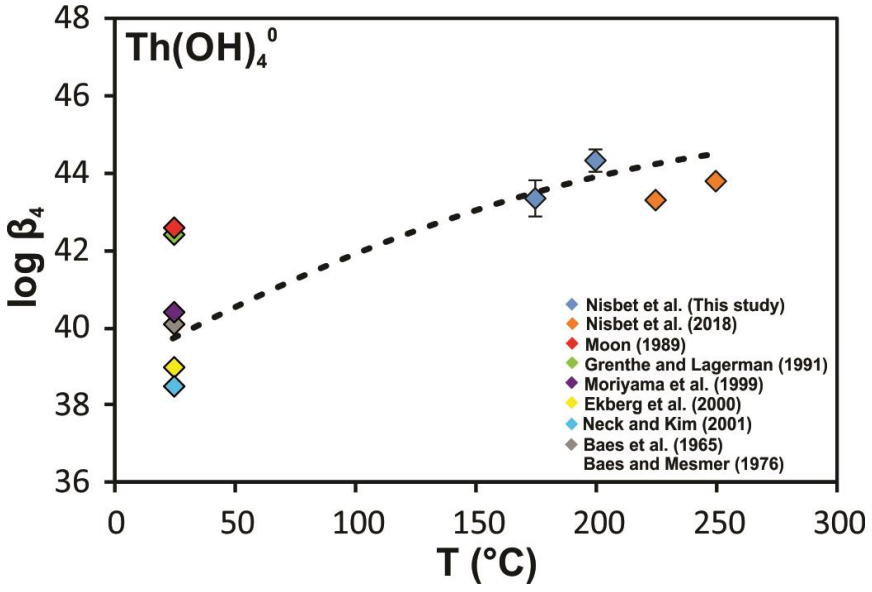

Figure 6. Thermodynamic formation constants for $Th(OH)_4^0$ from our previous study (225 and 250°C) (Nisbet et al., 2018) and values refined in the current study (175 and 200°C), extrapolated to 25 °C using the Ryzhenko-Bryzgalin model (dashed line). The error bars for 225 and 250°C are less than the

diameters of the symbols. Formation constants reported for 25°C from ambient temperature experiments are shown for comparison.

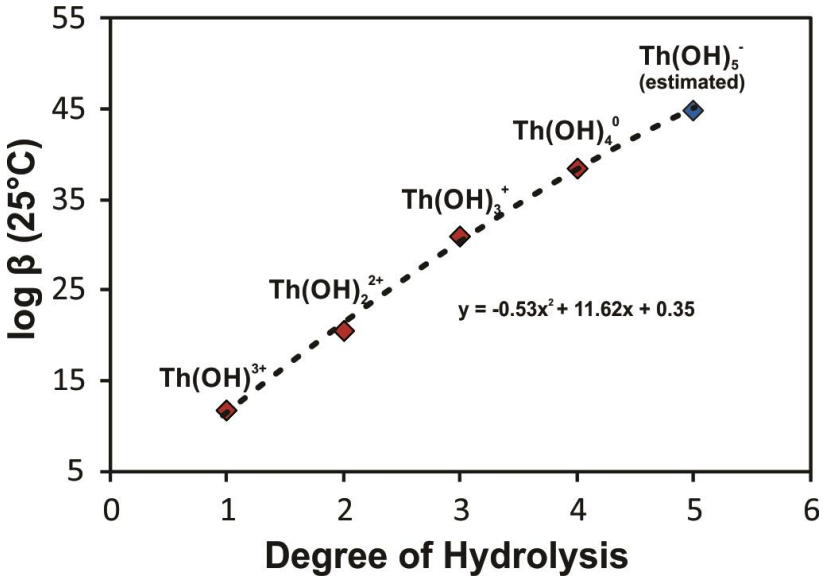

Figure 7. Thermodynamic formation constants for Th hydroxyl species at 25°C plotted as a function of the degree of hydrolysis. Data for $Th(OH)^{3+}$ and $Th(OH)_3^+$ was taken from Neck and Kim (2001), data for $Th(OH)_2^{2+}$ was taken from Nisbet et al. (2018) and the value for $Th(OH)_4^0$ is the value derived in this study. The equation of the polynomial fit was used to derive the formation constant of $Th(OH)_5^-$ at 25°C.

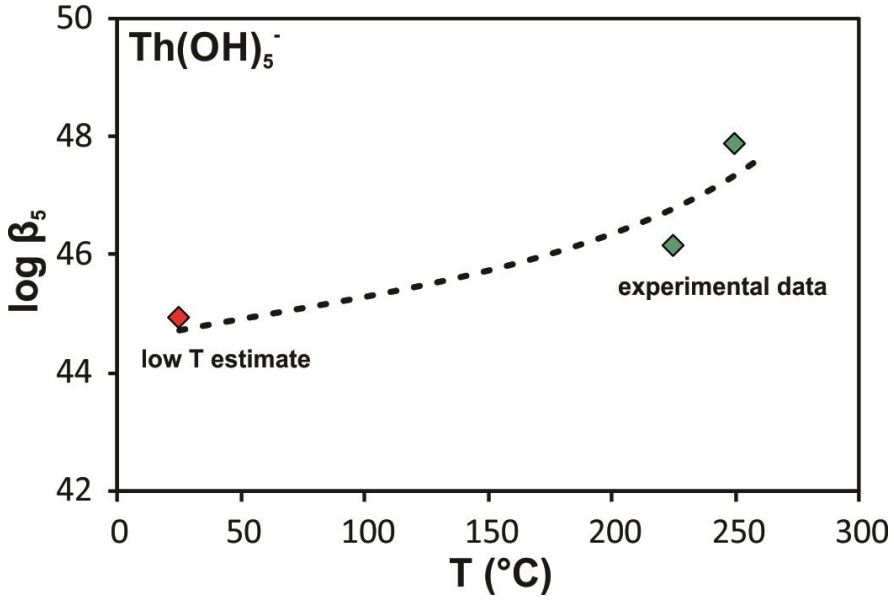

Figure 8. Thermodynamic formation constants for $Th(OH)_5^-$ derived in this study, and an estimate of the formation constant for this species at 25°C (as described in the text and illustrated in Figure 7) fitted to

the Ryzhenko-Bryzgalin model (dashed line). The error bars for the formation constants derived in this study are less than the diameters of the symbols.

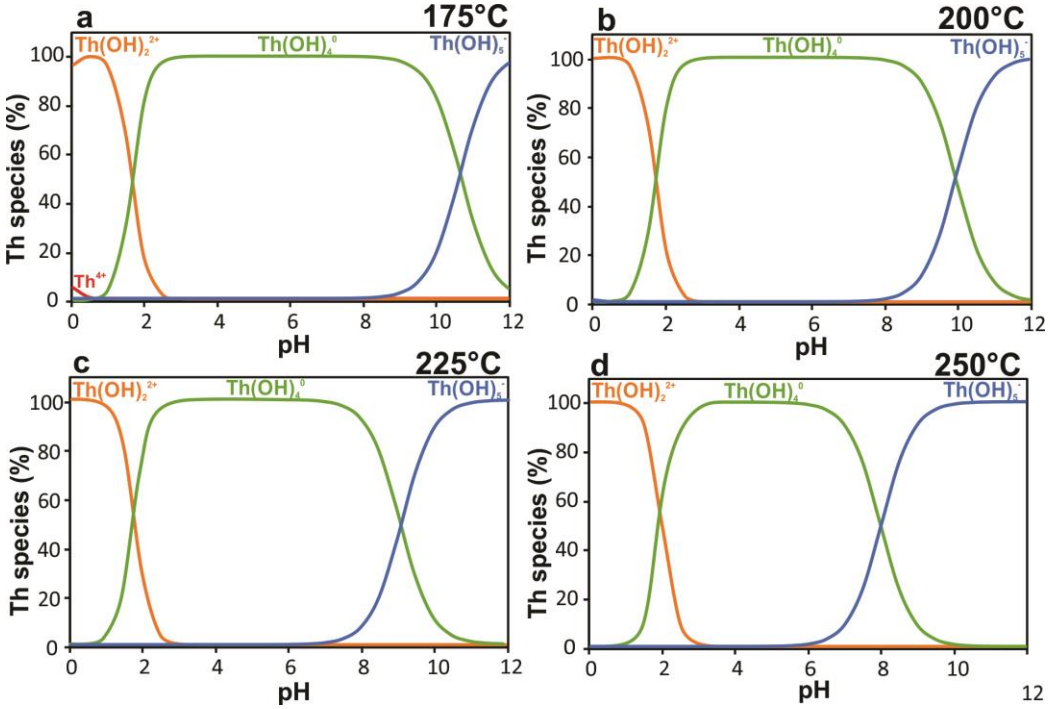

Figure 9a-d. Diagrams showing the proportions of the different Th-hydroxyl species as a function of pH at the temperatures investigated in this study: (a) 175°C, (b) 200°C, (c) 225°C, and (d) 250°C. The diagrams were constructed using thermodynamic data derived in this study and in Nisbet et al. (2018) studies.

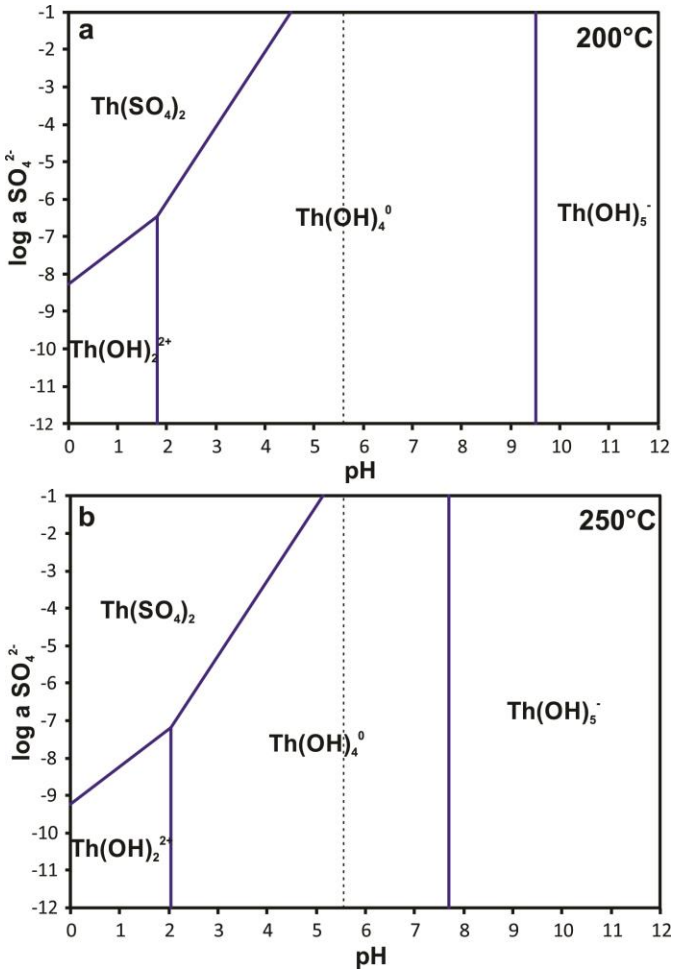

Figure 10. Diagrams showing the predominance fields of thorium aqueous species for (a) 200°C and (b) 250°C. The dashed line represents neutral pH at the respective temperatures. Data used to construct the diagrams were taken from Shock et al. (1997), Nisbet et al. (2018), Nisbet et al. (2019), and this study.

Tables

Table 1. The compositions of the experimental solutions in this study, the calculated activity of HCO_3^- and pH_T, the measured concentration of Th and the temperature. All experimental solutions contained 1m NaCl.

T (°C)	m $NaHCO_3$	m Na_2CO_3	log a HCO_3^-	pH_T	log m Th
175	0.05		-1.678	7.837	-6.695
175	0.1		-1.380	7.855	-6.568
175	0.15		-1.208	7.857	-6.726
175	0.25		-0.993	7.853	-6.690
175	0.3		-0.917	7.85	-6.609
175	0.35		-0.854	7.846	-6.398
175	0.4		-0.799	7.842	-6.826
175		0.05	-2.053	9.337	-6.791
175		0.15	-1.792	9.594	-7.272
175		0.2	-1.730	9.653	-6.890
175		0.25	-1.685	9.696	-6.909
175		0.4	-1.595	9.780	-7.173
175		0.45	-1.574	9.799	-6.972
175		0.5	-1.555	9.816	-6.849
200	0.15		-1.268	7.961	-5.501
200	0.2		-1.148	7.962	-5.855
200	0.25		-1.055	7.96	-5.876
200	0.3		-0.980	7.958	-5.584
200	0.35		-0.918	7.954	-5.685
200	0.4		-0.863	7.951	-5.304
200	0.45		-0.816	7.947	-5.764
200		0.15	-1.757	9.505	-6.311
200		0.25	-1.649	9.61	-5.824
200		0.3	-1.614	9.645	-6.392
200		0.35	-1.585	9.673	-6.021
200		0.4	-1.560	9.696	-6.120
200		0.45	-1.540	9.716	-5.988
200		0.45	-1.540	9.716	-6.547
225	0.05		-1.808	8.028	-6.125
225	0.10		-1.512	8.070	-6.485
225	0.15		-1.341	8.082	-6.254
225	0.20		-1.221	8.086	-6.414
225	0.25		-1.129	8.086	-6.046
225	0.30		-1.055	8.084	-6.449
225	0.35		-0.993	8.082	-6.297
225	0.40		-0.940	8.079	-6.771
225	0.45		-0.893	8.075	-5.912
225		0.05	-2.031	9.175	-5.065
225		0.10	-1.847	9.357	-4.802
225		0.15	-1.750	9.453	-4.871
225		0.25	-1.641	9.562	-4.993
225		0.30	-1.605	9.597	-5.151

225		0.40	-1.552	9.650	-4.997
225		0.45	-1.532	9.670	-4.975
225		0.50	-1.515	9.687	-4.758
250	0.15		-1.428	8.222	-5.675
250	0.20		-1.309	8.229	-5.543
250	0.25		-1.218	8.231	-5.900
250	0.30		-1.144	8.230	-5.493
250	0.35		-1.083	8.229	-5.407
250	0.40		-1.031	8.226	-5.937
250	0.45		-0.985	8.223	-5.438
250	0.05	0.05	-1.701	8.961	-5.190
250	0.075	0.075	-1.558	9.022	-5.247
250	0.1	0.1	-1.457	9.055	-4.925
250	0.15	0.15	-1.318	9.086	-4.882
250	0.175	0.175	-1.265	9.094	-4.941
250	0.2	0.2	-1.220	9.098	-5.232
250	0.225	0.225	-1.181	9.1	-5.404
250	0.25	0.25	-1.146	9.101	-5.139
250		0.05	-2.062	9.154	-4.820
250		0.1	-1.871	9.341	-4.650
250		0.15	-1.772	9.440	-4.745
250		0.2	-1.707	9.505	-4.827
250		0.25	-1.660	9.552	-4.530
250		0.3	-1.625	9.588	-4.693
250		0.35	-1.596	9.617	-4.690
250		0.45	-1.553	9.661	-4.536
250		0.5	-1.536	9.679	-4.742

Table 2. The composition of the time series experimental solutions and the measured concentration of Th collected sequentially over 14 days. All solutions contained 1m NaCl.

T (°C)	m $NaHCO_3$	Time (days)	log a HCO_3^-	pH_T	log m Th
175	0.25	0.94	-0.9932	7.853	-6.308
175	0.25	1.93	-0.9932	7.853	-6.203
175	0.25	2.93	-0.9932	7.853	-6.178
175	0.25	3.94	-0.9932	7.853	-6.142
175	0.25	6.92	-0.9932	7.853	-6.002
175	0.25	7.93	-0.9932	7.853	-5.823
175	0.25	13.93	-0.9932	7.853	-6.107

Table 3. The logarithm of the thermodynamic formation constants for $Th(OH)_4^0$ (log β_4) and $Th(OH)_5^-$ (log β_5) derived in this study.

	175°C	200°C	225°C	250°C
log β_4	43.34 ± 0.5*	44.31 ± 0.3*		
log β_5			46.15 ± 0.09	47.9 ± 0.1

**Revised from Nisbet et al. (2018)*

Table 4. Revised Ryzhenko–Bryzgalin (MRB) model parameters for $Th(OH)_4^0$ (from Nisbet et al., 2018)) derived from experimental data collected in this study at 175 and 200°C, and data collected by Nisbet et al. (2018) at 225 and 250°C.

	pK (298)	**A(zz/a)**	**B(zz/a)**
$Th(OH)_4^0$	39.769	-1.045	4139.69

Table 5. Estimated Ryzhenko–Bryzgalin (MRB) model parameters for $Th(OH)_5^-$.

	pK (298)	**A(zz/a)**	**B(zz/a)**
$Th(OH)_5^-$	44.713	6.987	0.00